

# Why is the slice rephaser just half the slice-selection gradient?

Olaf Dietrich\*, Munich

2025-03-27

Or, to use slightly more precise language: “Why is the area of the slice-selection rephasing gradient just half the area of the slice-selection gradient?” The meaning of this question is visualized in the following figure, which shows the initial part of a typical, but simplified slice-selective MRI pulse sequence with a radio-frequency (rf) pulse and the slice-selection gradient amplitude,  $G_z$  (it’s simplified because the gradients do not have a trapezoidal shape, but appear to be switched on and off infinitely fast):

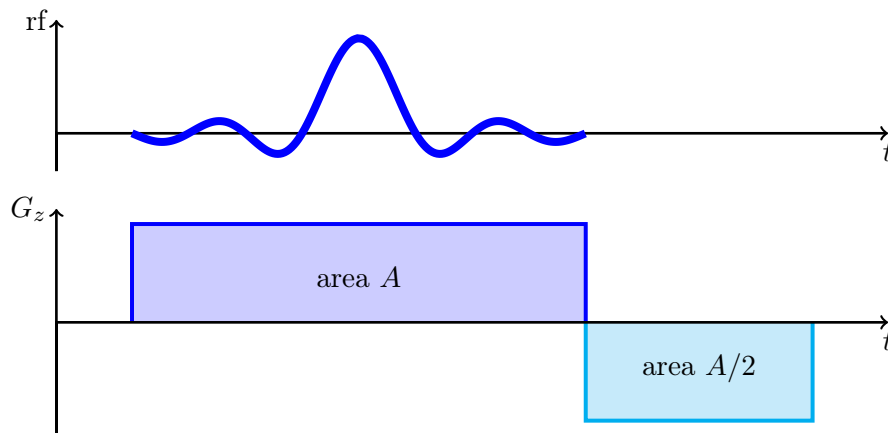


Figure 1: Slice-selection part of an MRI pulse sequence: Why is the light-blue area just half of the dark-blue area?

Some background explanations about slice selection in MRI can be found in two [earlier posts from 2017-12-15](#) and [2020-09-10](#). What I didn’t mention there is that the slice-selection gradient,  $G_z$ , dephases (as a kind of unwanted side effect) the spins *within* the selected slice: Due to the slice-selection gradient, the magnetic field varies linearly along the  $z$  (slice-selection) direction. Therefore, the precession frequency  $\omega(z) = \gamma(B_0 + zG_z)$  is different at different positions  $z$  within the selected slice, which means that the spins

---

\*Please send comments, corrections, or suggestions to [<olaf@dx.de>](mailto:olaf@dx.de).

dephase and the transverse magnetization (i. e., the signal) is destroyed. To compensate for this (and recover the signal), the (light-blue) rephasing gradient is required.

Over the last months, I was asked the initially cited question about the area of the slice-selection rephaser a few times, and after some discussions I had to admit that my usual explanation is not fully satisfying (or, maybe, not satisfying at all . . .).

My usual explanation was: Well, the details of rf excitation are complicated, but as a first approximation let's just assume that the excitation (e. g., the  $90^\circ$  flip of the magnetization) takes place *instantaneously at the center* of the rf pulse. So there is *no* dephasing before the center of the rf pulse and then there's "normal" gradient-induced dephasing (along the slice direction) afterwards; this dephasing is exactly rephased by the standard 50% rephasing gradient as in the diagram above.

And a completely justified reply to this is: Yeah, but the rf pulse has a certain duration and it should start turning the magnetization a bit out of the longitudinal direction as soon as it is switched on. So, dephasing should also start right away, shouldn't it? Then, why don't I need a full-size rephasing gradient (with the same area as the slice-selection gradient)?

At this point, I was running out of good and simple arguments . . .

But, of course, there should be *some* explanation (not necessarily a simple one), and to understand what's going on, it is always possible to simulate the effect of an rf pulse on some magnetization vectors and look at the dephasing and rephasing for some simple cases. So, let's do this now for three simple rf pulse shapes:

- A truncated sinc pulse (with 4 zeros on each side and Hann filter apodization) – this is a very typical rf pulse shape that has been used for years for slice-selective MRI, since it provides a nice, approximately rectangular slice profile (for more details see, e. g., the “[Handbook of MRI pulse sequences](#)” by Bernstein, King, and Zhou, chapter 2.2);
- a truncated Gaussian pulse (with a width of 3 standard deviations), which provides an approximately Gaussian slice profile (not ideal, but still usable for 2D imaging);
- a rectangular pulse (also called “hard” pulse), which is usually used only for non-selective excitation, since its sinc-like slice profile is not suited at all for slice-selective imaging. Nevertheless, this very simple pulse shape is really useful to learn something about the dephasing during excitation.

The following figure shows these three rf pulse shapes (in the top row, all with a total duration of 1 ms) and their frequency spectrum (blue in the bottom row, together with the FWHM bandwidth in gray). For small flip angles (e. g.,  $10^\circ$ ), the slice profile along the slice-selection direction will be approximately proportional to the shown frequency spectrum. As can be expected because of the different widths of the main lobes of the pulses in the time domain, their bandwidths are also quite different (note the different scales of the horizontal frequency axes).

Based on these pulse shapes, the actual rf pulse is obtained by multiplying an rf field with carrier frequency  $\omega_{\text{rf}}$  by these shapes. The carrier frequency is given by the field strength at the center,  $z_0$ , of the desired slice, i. e.,  $\omega_{\text{rf}} = \gamma(B_0 + z_0 G_z)$ .

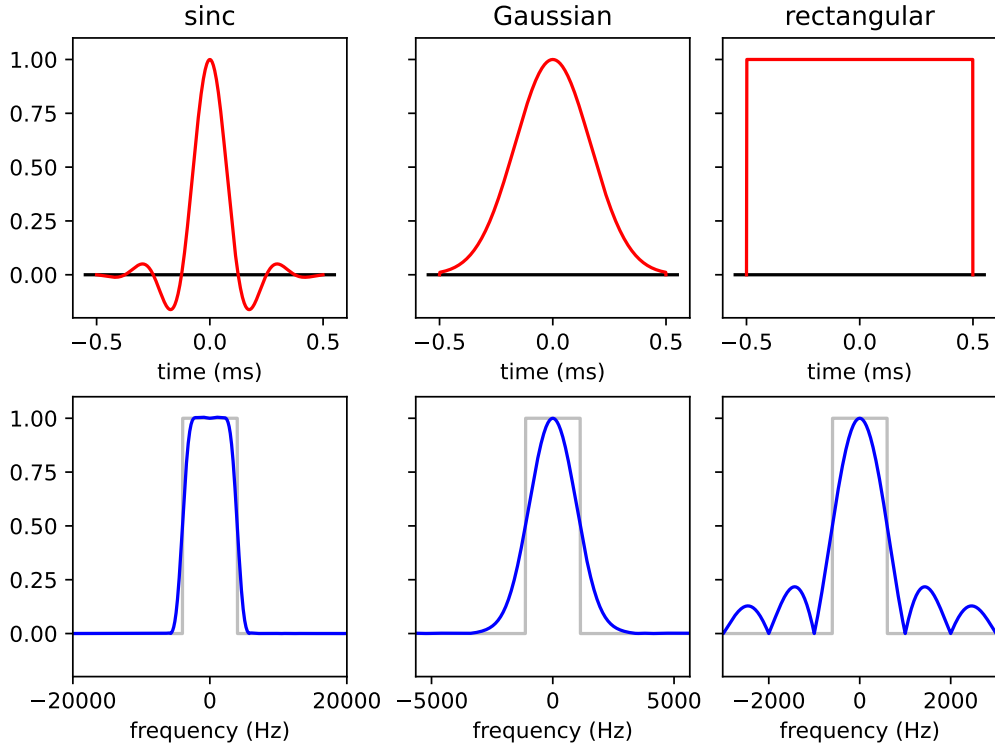


Figure 2: Three different rf pulse shapes, left: truncated sinc, center: truncated Gaussian, right: rectangular (hard) pulse. Top row: envelope in the time domain, bottom row: frequency spectrum (and FWHM).

Now let's simulate some magnetization vectors that are to be flipped by these three pulses by  $90^\circ$ . That's rather boring if we consider only the magnetization exactly at the center,  $z_0$ , of the excited slice where the precession frequency,  $\omega(z_0)$ , of the magnetization is exactly on-resonance (i. e., exactly the carrier frequency,  $\omega_{\text{rf}}$ , of the rf pulse). But if we look at spins that are still inside the excited slice, but positioned slightly off-center at  $z = z_0 + \Delta z$ , then their precession frequency will be different from the carrier frequency by  $\Delta\omega = \gamma\Delta z G_z$ . This difference is the reason for the dephasing that needs to be undone after the excitation.

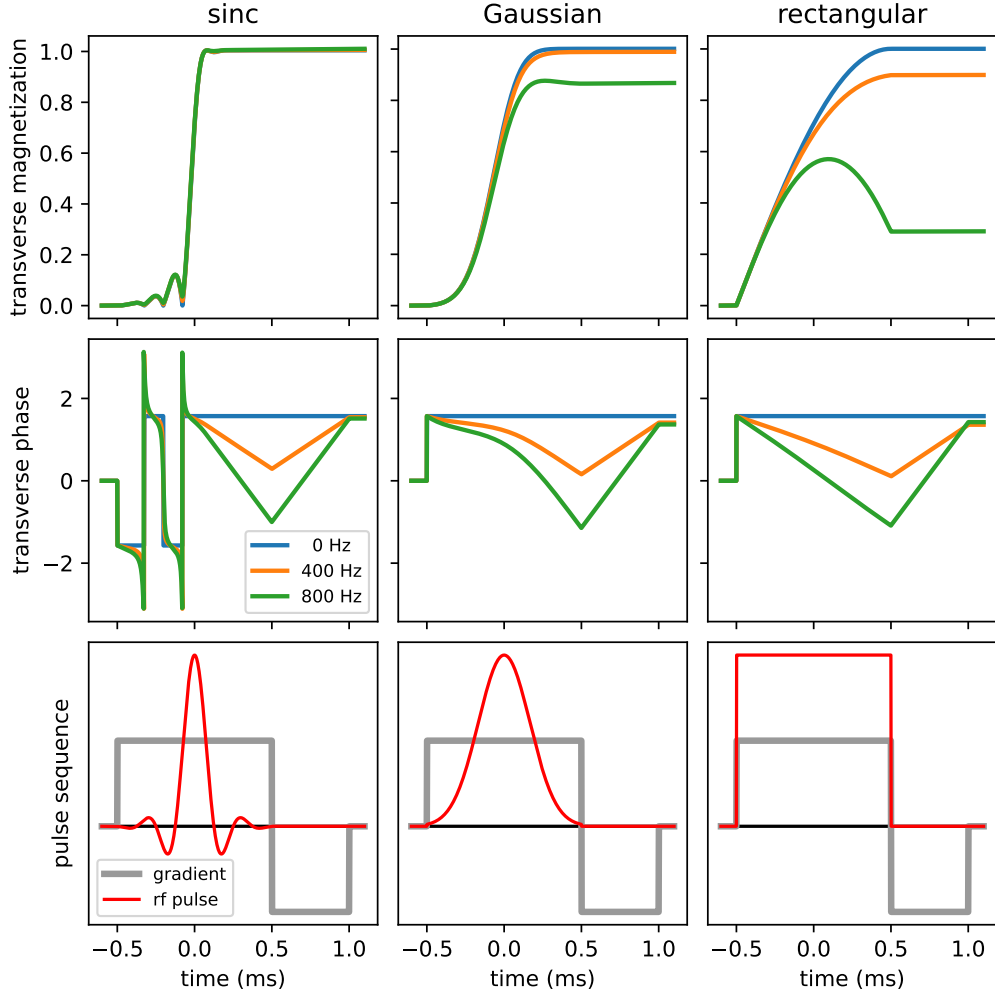


Figure 3: Simulation results with three different rf pulse shapes (sinc, Gaussian, rectangular) and three different frequency offsets of the magnetization vectors relative to the carrier frequency  $\omega_{\text{rf}}$  (blue:  $\Delta\omega = 0$  Hz, no offset; orange:  $\Delta\omega = 400$  Hz; green:  $\Delta\omega = 800$  Hz)

Perhaps surprisingly, the effect of the sinc pulse is that the resulting transverse magnetization (top row of the previous figure) is generated rather quickly around the center of the rf pulse (i. e., at  $t = 0$  ms); the magnetization can be well approximated by a step function and is almost independent of the frequency offset (which corresponds to the almost rectangular frequency spectrum). With the Gaussian pulse, the spin flip appears less instantaneous (less steep slope), and shows less efficient flipping for the highest frequency offset. Finally, with the hard pulse, the transverse magnetization builds up continuously over the total duration of the pulse (except for the highest frequency offset, which behaves more irregularly).

Even more interesting is the central row of the previous figure that shows the phase

evolution of the transverse magnetization (and, hence, contains the “simulation answer” to the original question). With the sinc pulse, there are some strange phase oscillations during the first half of the rf pulse ( $t \leq 0$  ms), but then – starting at a value of  $\pi/2$  – the magnetization dephases approximately linearly during the second half of the rf pulse ( $0 \leq t \leq 0.5$  ms) and rephases after the rf pulse ( $0.5 \text{ ms} \leq t \leq 1.0$  ms), when the rephasing gradient is switched on. Apparently, in this case, the phase of the spins does actually behave quite similar to my initial explanation . . .

However, the evolution is quite different with the Gaussian pulse: The dephasing starts immediately as soon as the rf pulse begins (at  $t = -0.5$  ms), slowly at the beginning, and then increasingly faster. At the end of the rf pulse, the resulting dephasing is approximately the same as for the sinc pulse and is almost completely rephased by the rephasing gradient.

Perhaps the most clarifying result is obtained with the rectangular pulse: The phase evolution is approximately linear during the rf pulse (starting simultaneously with the pulse), and the slope of the evolution is *half* of the slope (with opposite sign) seen during the rephasing gradient. So, the dephasing takes place over the whole duration of the rf pulse, but is exactly half as fast as the rephasing afterwards. Put differently: The effect of the slice-selection gradient is reduced by 50 % by the simultaneously acting rf pulse. And in my opinion, in this observation lies an alternative answer to the original question: During a constant rf pulse (independent of its amplitude), the dephasing takes place with half speed (compared to dephasing without rf pulse). During a non-constant, more complicate rf pulse (such as the sinc or the Gaussian pulses), the behavior is more complicated, but the result is about the same at the end of the pulse.

But *why* is the phase evolution slowed down to 50 % by the (constant) rf pulse? To see this, one needs to know a small factoid about the use of rotating reference frames in MR physics (that can be found, e. g., in the “[Handbook of MRI pulse sequences](#)” by Bernstein, King, and Zhou, chapter 1.2): The equation of motion for a magnetization vector,  $\mathbf{M}(t)$ , in a reference frame rotating with the carrier frequency,  $\omega_{\text{rf}} = \gamma(B_0 + z_0 G_z)$ , of the applied rf pulse is:

$$\left(\frac{d\mathbf{M}}{dt}\right)_{\text{rot}} = \gamma\mathbf{M} \times \left[ B_1(t)\mathbf{e}_x + \left( B_z - \frac{\omega_{\text{rf}}}{\gamma} \right)\mathbf{e}_z \right] \quad (1)$$

where  $B_1(t)$  is the envelope of the rf pulse and  $B_z = B_0 + zG_z$  is the static magnetic field strength at the position of the magnetization.

In the center of the excited slice at  $z = z_0$ , we have  $B_z = B_0 + z_0 G_z = \omega_{\text{rf}}/\gamma$ , which means that the equation of motion simplifies to  $d\mathbf{M}/dt = \gamma\mathbf{M} \times B_1(t)\mathbf{e}_x$ . This yields the precession of  $\mathbf{M}$  around the  $x$  axis as illustrated here:

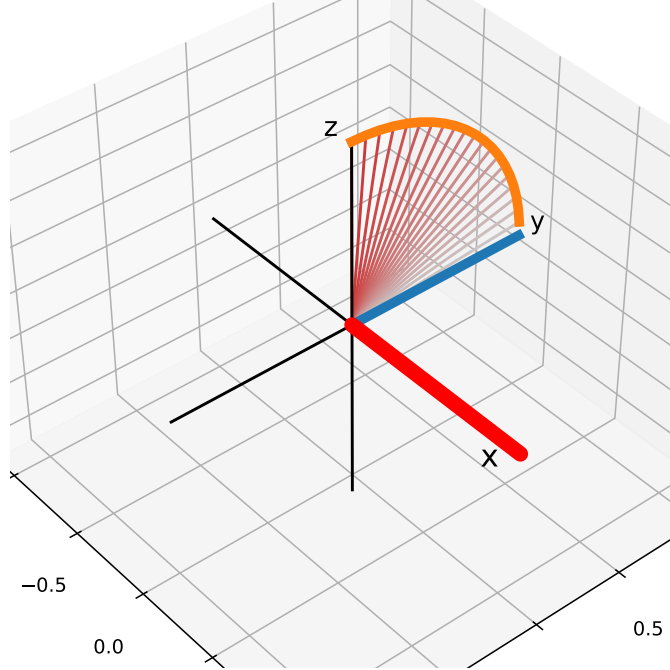


Figure 4: Simulated 3D trajectory (orange) of a magnetization vector precessing **with the carrier frequency**,  $\omega_{\text{rf}}$ , shown in a rotating reference frame. The magnetization is turned from the vertical  $z$  axis to the horizontal  $y$ -axis (the orange trajectory lies in the  $yz$  plane). The direction of the  $B_1$  field (constant in the rotating frame) is shown in red. The projection of the trajectory onto the transverse ( $xy$ ) plane is shown in blue.

The  $B_1$  vector is shown in red, pointing along the  $x$  axis, and the magnetization is turned from the longitudinal ( $z$ ) axis by  $90^\circ$  around this vector to the  $y$  axis (orange trajectory). The projection of the trajectory onto the transverse plane is shown in blue. There is no phase evolution (i. e., the polar angle in the transverse plane stays constant along the blue trajectory).

However, if we look at a magnetization vector at a different position  $z = z_0 + \Delta z \neq z_0$ , then we have  $B_z = B_0 + zG_z$ , resulting in a so-called *effective* field vector appearing in the brackets of the displayed equation of motion above. This effective field vector has two components, lying in the  $xz$  plane, namely  $(B_1, B_z - \omega_{\text{rf}}/\gamma) = (B_1, \Delta z G_z)$ . The direction of this effective field is shown in red again in the following figure, and the solution of the equation of motion is a precession of the magnetization around this new effective field:

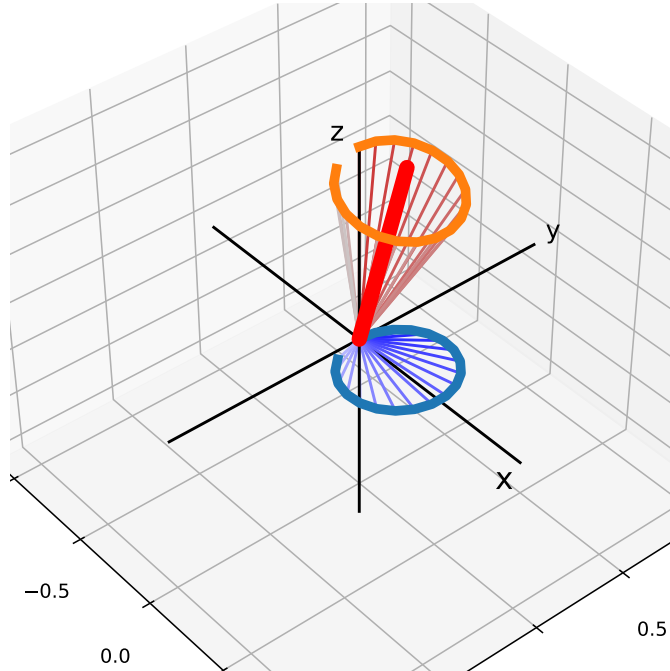


Figure 5: Simulated 3D trajectory (orange) of a magnetization vector precessing **with a frequency offset**  $\Delta\omega = \gamma\Delta zG_z$ , shown in a rotating reference frame. As before, the magnetization is initially oriented along the vertical  $z$  axis. The direction of the effective field is shown in red. The projection of the trajectory onto the transverse ( $xy$ ) plane is shown in blue.

The projection of the orange trajectory onto the transverse plan shows that **the 360° precession around the red effective field vector corresponds to a phase evolution by 180° in polar coordinates** (the thin blue vectors rotate basically once from the positive to the negative  $y$  axis, i. e., by 180°). This geometrical effect explains the 50 % reduction of the dephasing speed during the (constant) rf pulse. (To illustrate this effect, I've used a very large off-resonance frequency  $\Delta\omega = \gamma\Delta zG_z$  here, which means that the red  $B_1$  vector is turned very far out of its original direction and that the magnetization is no longer tilted by 90° at the end of the rf pulse. The same effect with respect to the (blue) polar angle would be found for smaller off-resonance frequencies, but would be harder to visualize.)

So, in the end we have two complementary explanations (illustrated in the third figure above) for the area under the slice-selection rephasing gradient:

- For rf pulse shapes such as truncated sinc pulses, the highest pulse amplitudes are found at the center of the pulse in the central lobe of the sinc function. The actual tipping of the magnetization occurs in this central part of the pulse; the effects of the long preceding and trailing parts of the amplitude on the phase evolution are mostly canceled by the positive and negative components of the shape there. For these pulses, assuming an approximately instantaneous spin flipping at the center

of the pulse is well justified by the simulation results.

- For simpler pulse shapes (without oscillations of the sign such as the Gaussian or rectangular pulses), the (monotonic) dephasing starts indeed immediately at the beginning of the pulse. However, the dephasing takes place (at least in average) with only *half* the precession frequency that one would expect for the given gradient, which means that at the end of the pulse the dephasing angle has only 50 % of the expected value.

Both explanations lead to the same area of the rephasing gradient, which is – in these cases – 50 % of the area of the slice-selection gradient.

*Keywords: MRI, pulse sequences, physics*